A New Strategy for Designing Conjugated Polymer-Based Fluorescence Sensing Films via Introduction of Conformation Controllable Side Chains

ARTICLE *in* MACROMOLECULES · JANUARY 2011

Impact Factor: 5.8 · DOI: 10.1021/ma102769b

7 AUTHORS, INCLUDING:

Gang he
Chengdu University
14 PUBLICATIONS **378** CITATIONS
SEE PROFILE

Shiwei Yin
Shaanxi Normal University
88 PUBLICATIONS **2,389** CITATIONS
SEE PROFILE

Liping Ding
Shaanxi Normal University
50 PUBLICATIONS **957** CITATIONS
SEE PROFILE

Yu Fang
Shaanxi Normal University
156 PUBLICATIONS **2,563** CITATIONS
SEE PROFILE

Macromolecules
ARTICLE

Macromolecules **2011**, *44*, 703–710 **703**
DOI: 10.1021/ma102769b

A New Strategy for Designing Conjugated Polymer-Based Fluorescence Sensing Films via Introduction of Conformation Controllable Side Chains

Gang He,[†] Ni Yan,[†] Hongyan Kong,[‡] Shiwei Yin,[†] Liping Ding,[†] Shixian Qu,[‡] and Yu Fang*,[†]

[†]*Key Laboratory of Applied Surface and Colloid Chemistry* (*Shaanxi Normal University*), *Ministry of Education, School of Chemistry and Materials Science, Shaanxi Normal University, Xi'an 710062, P. R. China, and* [‡]*School of Physics and Information Technology, Shaanxi Normal University, Xi'an 710062, P. R. China*

Received May 31, 2010; Revised Manuscript Received January 3, 2011

ABSTRACT: A fluorescence behavior controllable conjugated polymer (CP)-based fluorescent film was developed by chemical attaching poly(2,5-dihexadecyloxyphenyleneethynylene) (M-PPEs) onto a glass plate surface. It was revealed that the profile of the fluorescence emission spectrum of the film depended upon the polarity of its medium. This dependence has been attributed to the alteration of the conformation of the side chains of the polymer in immobilized state. In "poor" solvents or vapors, the side chains may adopt a compact coil conformation, resulting in aggregation of the immobilized polymers, and thereby fluorescence emission of the film is reduced because of the so-called aggregation-induced fluorescence quenching effect. Whereas in "good" solvents or vapors, the side chains tend to be swollen and adopt extended or loose coil structure, thereby preventing aggregation of the polymers, coupled with increasing of the fluorescence emission. Interestingly, this alteration process is fully reversible, and the retention time for each equilibration is less than 1 min. The film is also responsible for the changes in the compositions of mixture solvents, such as THF/methanol. In particular, two-input INH and OR logic gates were presented on the basis of the film. No doubt, this finding can be taken as a new strategy for the design of CPs and self-assembled monolayer (SAM)-based fluorescent sensing films and will definitely expand their applications.

Introduction

Surface functionalization plays a great role in the production and creation of electronics, catalysts, chemical sensors, and nanoscale- and molecule-level devices.[1] Presently, much attention has been devoted to modulating the microstructures of chemical assembled surfaces and the functional properties of SAM-based films.[1d,2] Tailoring of interface or surface-confined phenomena requires precise control of such interface or surface with predefined structures. For advanced applications, reversible external alteration of the interface or surface structures is a necessity.[3]

Recently, fluorescent sensing films via chemical assembly of low-molecular-weight fluorescent compounds on the functional terminus of surface-supported surfaces have received a great deal attention, mainly because this methodology offers several advantages in generating sensing films: (1) fast response based on the design strategy of directly exposing fluorophores to the testing solution, (2) high stability coming from the chemical bond among the components, (3) diverse film structures by varying the combinations of spacers, fluorophores and substrates, and (4) multiple measurable photophysical parameters.[1c,4] Such a strategy was extensively utilized by both Reinhoudt and co-workers and our group in developing fluorescent SAM sensors and exploring their potential applications. These fluorescent films have been reported to be sensitive and selective to the presence of metal cations, neutral chemicals, and even organic metal salts.[5,6] Interestingly, the interface or surface properties of these films have been proved to be regulable not only by means of changes in the nature of the functional molecules or their geometry but also by the conformational changes in the spacers connecting the fuorophores and the substrate, which plays a great role in mediating the fluorescence sensing properties.[7]

Compared to these small-molecule fluorophores, conjugated polymers (CPs) or oligomers are not only fluorescence active but also possess the so-called superquenching effect since their backbone can act as a molecular wire, enabling the rapid propagation of an exciton throughout the individual polymer chain.[8] Although CPs have been extensively utilized in preparing highly sensitive film sensors, most of the reported work has been limited to using spin coating or casting to prepare CP films.[9] Our group started to explore the combination of CPs and SAM technique to prepare highly sensitive and stable film sensors a few years ago.[6] On the basis of the strategy, several CPs-based film sensors have been prepared and exhibited excellent responses for nitro-aromatic compounds (NACs) either in vapor or in solution and formaldehyde vapor.[10] Just following the philosophy that "everything is divided into two", utilization of CPs as fluorescent sensing elements brings SAMs-based fluorescent films superior sensitivity, but coupled with difficulties in immobilization of the CPs and in varying the structures of the spacers connecting the CPs and the substrate, which seriously limits the creation of more fluorescent film sensors based on SAMs and CPs. Therefore, new strategies for creation of this type of fluorescent film sensors with superior performances are desperately needed.

Considering the facts that CPs are "rigid" molecules[11] and their fluorescence behaviors depend upon their physical states, it is reasonable to presume that variation in the conformation of the side chains of a CP may result in changes of the photophysical property of such a CP-functionalized fluorescent SAM.[12] To prove the feasibility of such a concept, a long flexible alkyl, hexadecyl, was introduced as side chains of poly(*p*-phenyleneethynylene) (PPEs) in fabricating a PPE-functionalized film sensor.

*Corresponding author: e-mail yfang@snnu.edu.cn; Tel 0086-29-85300081; Fax 0086-29-85307566.

Published on Web 01/20/2011

Scheme 1. Schematics for the Synthesis of PPEs and Its Coupling onto a Glass Plate Surface

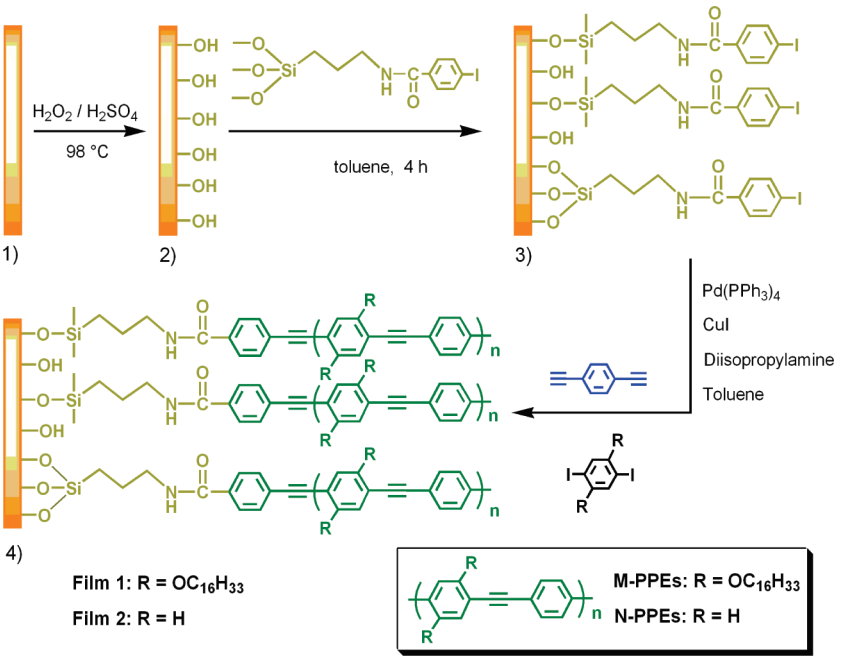

Experimental Section

Materials. Diphenylacetylene (Acros, 97%), (3-aminopropyl)trimethoxysilane (Alfa Aesar, 97%), 4-iodobenzoyl chloride (Alfa Aesar, 98%), 1,4-diiodobenzene (Alfa Aesar, 98%), $Pd(PPh_3)_4$ (Alfa, 99%), and CuI (Alfa, 98%) were used as received. All manipulations for the preparation of the samples were performed using standard vacuum line and Schlenk techniques under a purified argon atmosphere. THF and toluene were distilled from sodium benzophenone ketyl under argon prior to use. 1,4-Dihexadecyloxy-2,5-diiodobenzene and 4-iodo-*N*-3-(trimethoxysilyl)propyl benzamide were synthesized according to a literature method.[13,14] All manipulations for the preparation of the samples were performed using standard vacuum line and Schlenk techniques under a purified argon atmosphere.

Instruments. Both steady-state and time-resolved fluorescence measurements were performed at room temperature on a time-correlated single photon counting Edinburgh FLS 920 fluorescence spectrometer with a front-face method. The fabricated film was inserted into a quartz cell with its surface facing the excitation light source. The cell was fixed in the solid sample holder of the instrument. The position of the film was kept constant during each set of measurements. Contact angles of the films were measured on a dataphysics OCA20 contact-angle system at ambient temperature. X-ray photoelectron spectroscopy (XPS) measurements were carried out on an ESCA-PHI5400 photoelectron spectrometer using a monochromatic Mg Kα X-ray source. The ellipsometric thicknesses of the layers on glass plate substrate were measured on SpecEl-2000-VIS spectroscopic ellipsometer (Mikro Pack). ^{1}H NMR spectra were measured on Bruker AV 300 NMR spectrometers. GPC was performed at 35 °C using THF as the eluent at a flow rate of 1.0 mL min^{-1}. The GPC instrument was equipped with a Waters 717 plus autosampler, a Waters 1515 HPLC pump, three μ-Styragel columns, and a Waters 2414 refractive index (RI) detector. The columns were calibrated using polystyrene standards.

Activation and Silanization of the Glass Plate Surface. A glass plate (0.9 cm × 2.5 cm) was treated in a "piranha solution" (7/3, v/v, 30% H_2O_2/98% H_2SO_4)[15] (*warning: piranha solution should be handled with extreme caution since it can react violently with organic matter*) at 98 °C for 1 h, then rinsed thoroughly with plenty of water, and finally dried at 100 °C in a dust-free oven for 1 h. The activated glass plate was placed in flask charged with a toluene solution (20 mL) of 4-iodo-*N*-3-(trimethoxysilyl)propylbenzamide (0.67%, v/v), and the solution was refluxed for 4 h. After cooling to room temperature, the plate was removed from the flask, successively washed with a copious amount of toluene and ethanol, and then dried under a gentle stream of nitrogen.[14]

Chemical Coupling of M-PPEs onto a Glass Plate Surface. Chemical coupling of poly(dihexadecyloxyphenyleneethynylene) (M-PPEs) on a glass plate surface was performed using solution step-growth polymerization reaction.[14] 1,4-Diethynylbenzene (25 mg, 0.2 mmol), 1,4-dihexadecyloxy-2,5-diiodobenzene (159 mg, 0.196 mmol), CuI (1.86 mg, 9.8 μmol), and $Pd(PPh_3)_4$ (11.3 mg, 9.8 μmol) were dissolved in a mixture of 14 mL of toluene and 6 mL of diisopropylamine. The mixture was heated at 70 °C for 24 h, and ammonium iodide was formed immediately. The mixture is highly fluorescent, and the color of the emission turns from blue to green along with the progress of the reaction. After cooling the mixture to room temperature, the functionalized film was removed and washed with plenty of toluene and ethanol. The free polymers within the reaction mixture were precipitated by dropwise addition of the mixture into plenty of acetone (400 mL) under vigorous stirring. The precipitate (M-PPEs) was collected and washed repeatedly with acetone, hot ethanol, and *n*-hexane and then dried overnight at 50 °C. M_n = 1.94 × 10^4 by GPC (PDI = 1.53). ^{1}H NMR ($CDCl_3$) d 7.54 (br, 4H), 7.34 (d, 2H), 7.02−7.00 (m, 2H), 3.92 (m, 4H), 1.79 (br, 4H), 1.49 (br, 4H), 1.26 (br, 48H), 0.88 (t, 6H). The stability of this film in THF was confirmed by monitoring the fluorescence emission as a function of time (cf. Figure S1). The side-chain-free polymer, poly(phenyleneethynylene) (N-PPEs), functionalized film was fabricated in a similar way. The films fabrication process is shown in Scheme 1.

Results and Discussion

Characterization of the Films. The films have been characterized by XPS, wettability, and thickness measurements. Figure 1 shows the XPS spectra of the substrate of various surface compositions, of which the chemical structures changed from hydroxyl groups, aryl iodide groups, to M-PPEs or N-PPEs along with the treatments (cf. Scheme 1). It can be seen that the signal of C 1s became much stronger, and the

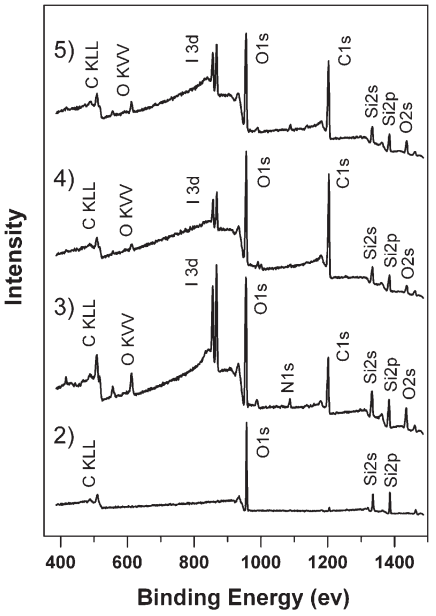

Figure 1. X-ray photoelectron spectra of the glass plates of various surface structures: (2) plate with activated surfaces, (3) plate with an aryl iodide surface, (4) plate with a M-PPEs-coated surface, and (5) plate with a N-PPEs-coated surface.

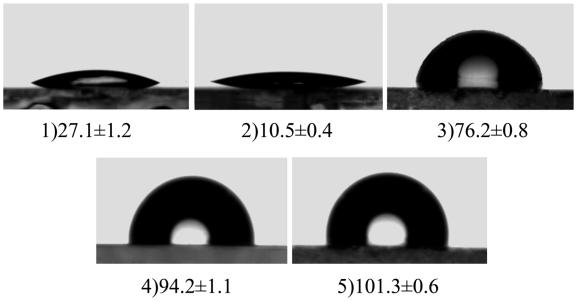

Figure 2. Advancing contact angles (θ) of various glass plate surfaces to water: (1) the original clean glass plate, (2) plate with activated surfaces, (3) plate with an aryl iodide surface, (4) plate with a M-PPEs-coated surface, and (5) plate with a N-PPEs-coated surface.

signals of N 1s and I 3d appeared after silanization, a direct evidence for the successful coupling of the silanizing reagent on the glass plate surface. Immobilization of M-PPEs on the surface made C 1s signal even stronger, while the signals of I 3d became significantly weaker due to reaction of the end iodine groups, an indication of successfully coupling of M-PPEs (cf. Figure 1). The corresponding conversion efficiency is about 35%, which was calculated by using the XPS data according to a method reported by our group earlier.[10b] Nevertheless, remain of the weak I 3d signal in the final film indicates that the reactive sites on the glass plate surface had not been fully occupied by the conjugated polymers. Coupling of M-PPEs on the substrate surface was further confirmed by the results from surface wettability measurement.

Contact angles (θ) of the surfaces of the substrate to water at ambient temperature were monitored at different stages of the functionalization process, and the results are shown in Figure 2. Reference to the figure reveals that the contact angles decrease significantly from 27.1 ± 1.6° to 10.5 ± 0.4° after activation with the "piranha solution". Further treatment with 4-iodo-*N*-3-(trimethoxysilyl)propylbenzamide results in a sharp increase in the data (76.2 ± 0.8°), indicating that the wettability of the surface has reversed. The angle

Table 1. Ellipsometric Thickness of the Fluorescent Films on Oxidized Silicon Wafer

samples	thickness (±0.5), Å
glass plate with iodine surface	24
glass plate with M-PPEs-coated surface	143

increases further with the introduction of M-PPEs or N-PPEs and reaches a value of 94.2 ± 1.1° or 101.3 ± 0.6°, typical hydrophobic surfaces. These results are consistent with the expectation from the chemical compositions of the surfaces, as shown in Scheme 1 and revealed by XPS measurement.

Ellipsometry is a widely used optical technique for measuring the thickness of thin films. In this study, the measurements of the layers were made on glass plate assuming a refractive index of 1.5 for the layer over the substrate surface. Average values for the adlayers are summarized in Table 1. It is clear that the adlayer with iodine as their end groups are not true monolayer because the thickness (24 Å) measured is much thicker than that predicated theoretically by calculating the molecular length of 4-iodo-*N*-3-(trimethoxysilyl)propylbenzamide and angles of the chemical bonds in the silanizing reagent. The difference between the experimental result and that predicted may be attributed to the use of trialkoxysilane as a coupling reagent, which is known to form polysilanols readily, resulting in multilayer structures on the surface. After coupling M-PPEs, the thickness of the film increased to 14.3 nm, a net increase of 11.9 nm, which is a value significantly shorter than 18 nm, a theoretical data obtained by modeling the oligomer with Materials Studio 3.0. This is not a surprising result considering that M-PPEs could not stand perpendicularly on the substrate surface.

Steady-State Excitation and Emission Spectra of the Film. The excitation and emission spectra of both the long-alkyl-side-chain-modified PPEs (M-PPEs) in THF and film based upon M-PPEs (film **1**) in dry state are shown in Figure 3. The maximum excitation of M-PPEs in THF appeared at 415 nm, and the emission centered at 445 nm with a shoulder appeared at 475 nm. Whereas, as to film **1** in dry state, its maximum emissions shifted to 465 and 510 nm, respectively, and the emission centering at 510 nm is broader and stronger than that peaking at 465 nm. The variation in the position and profile of the emission spectra might be originated from variation of the conformation of M-PPEs in different microenvironments. The emission appearing at longer wavelength should be the one from aggregated state and the other at shorter wavelength from free monomolecular state. Thus, the molecules of M-PPEs on the film in dry state are mainly aggregated because their emission is dominated by the longer wavelength emission. In contrast, in solution state, they prefer to stay in monomolecular state. The loading density of fluorophore on the substrate surface was determined by a literature method,[6b,16] and the result is ~28% (1.6 molecules per 100 Å^2) relative to the theoretical value (5.8 molecules per 100 Å^2). The aggregation phenomenon of M-PPEs was carefully studied in miscible solvents by steady-state and time-resolved fluorescence techniques, which confirmed that it is the aggregation that resulted in the change in the profiles of the fluorescence emission spectra.

Aggregation of M-PPEs in Mixture Solvents. To investigate the aggregation behavior of M-PPEs in solution, miscible solvents were employed to adjust the solubility of the polymer in the solvents. For M-PPEs, THF is a "good" solvent, but ethanol and water are "poor" solvents. Accordingly, the fluorescence emission spectra of M-PPES in THF−ethanol mixtures were recorded, and the results are

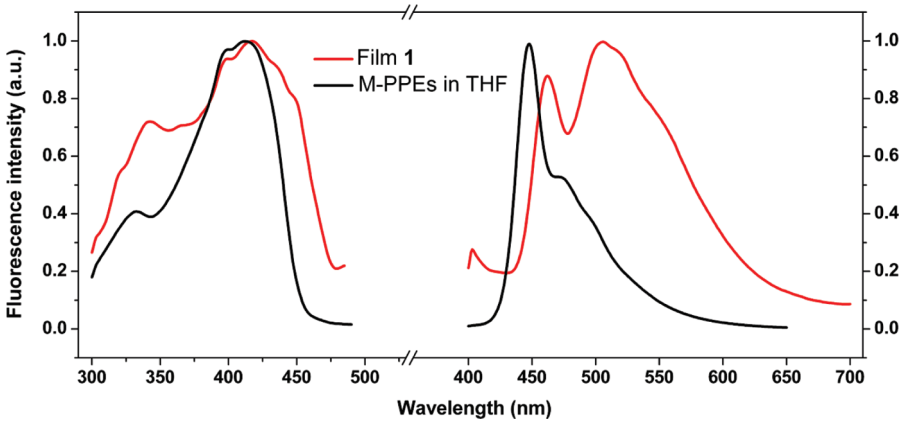

Figure 3. Excitation and emission spectra of M-PPEs in THF and film **1** in dry state (λ_{ex} = 415 nm, λ_{em} = 500 nm).

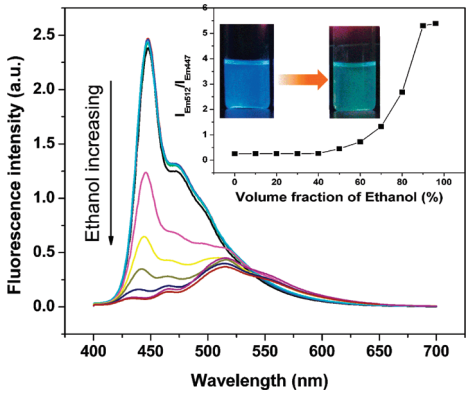

Figure 4. Fluorescence emission spectra of M-PPEs in THF:ethanol (v:v) (λ_{ex} = 380 nm). Insets are the photos of the emission under UV irradiation and the composition dependence of the ratio of the emission intensity centered at 512 nm and that centered at 447 nm.

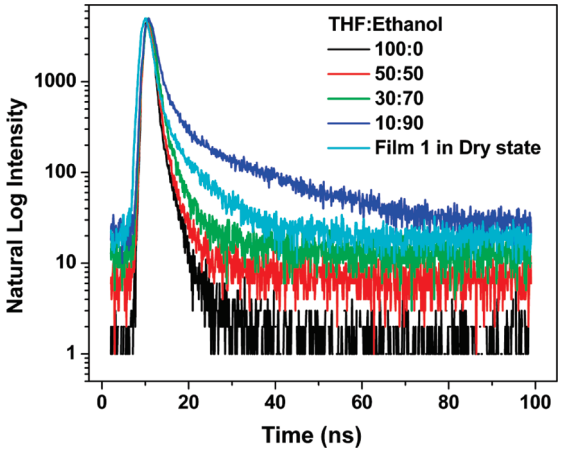

Figure 5. Semilog plots of fluorescence intensity vs time for M-PPEs in THF:ethanol mixtures of different compositions and that in dry film state (λ_{ex} = 380 nm, λ_{em} = 500 nm).

presented in Figure 4. It can be seen that M-PPEs in pure THF shows a blue emission under UV irradiation, but in contrast the emission turns to green when the composition of the mixture solvents is dominated by ethanol (cf. inset of Figure 4). Reference to the emissions shown in the figure reveals that the emission is dominated by the one centering at 445 nm or within 430−460 nm when the content of ethanol in the mixture does not exceed 50% (v/v). Further addition of ethanol to the mixture is accompanied by a decrease in the blue emission, an indication of inner-filtering effect resulted from aggregation of the polymers, a well-reported aggregation induced fluorescent quenching phenomenon for conjugated organic polymers.[17] Meanwhile, green emission (500−530 nm) is becoming significant, not due to its increase but due to the decrease of the blue emission. It is worth well to mention that the aggregates of the polymer formed in the mixture solvent can be observed directly by the naked eye (cf. Figure S2). Interestingly, the profile of the emission of film **1** in dry state is similar to that of M-PPES in a specific THF:ethanol mixture (3:7) (cf. Figure S3), suggesting that the packing degree of M-PPEs in immobilized state is close to that of the polymer in the mixture solvent.

Furthermore, the aggregation behavior of the polymer in another mixture of solvents, THF:water, was also studied, and the results are shown in Figures S4 and S5. The details are described in the relevant section of the Supporting Information.

Fluorescence Lifetime Measurements. Fluorescence lifetime of a conjugated polymer in monomolecular state should be very different from that in aggregated state, and thereby, the aggregation of M-PPEs in the mixture solvent can be also interrogated by conducting lifetime measurements. Figure 5 depicts the fluorescence decays of M-PPEs in THF:ethanol of different compositions and that in dry film state. Reference to the figure reveals that the decay depends upon the composition of the mixture solvent. Clearly, the decay is becoming slower and slower with increasing the ratio of ethanol in the mixtures. The average lifetime of the polymer in the mixture solvent increased from 1.21 to 1.54 ns with increasing ethanol from 0 to 70% (v/v). Furthermore, the decays could be reasonably fitted by using a double-exponential function. For comparison, the fluorescence decay of film **1** in dry state was also recorded. Reference to the decays, it is seen that the decay of film **1** is close to one of the M-PPEs' decays recorded in its THF−ethanol mixture solvents, of which the ratio of THF to ethanol is 3 to 7, indicating again that M-PPEs in the two systems have aggregated in a similar way and a similar level provided the substrate shows little effect to the decay process, which is the main reason for people to adopt silica as a substrate.[18] Once the presence of the aggregate both in mixture solvent and in immobilized state was confirmed, the next step is to determine whether the aggregate is formed prior to the excitation (static aggregate) or after the excitation (dynamic aggregate, forms via a mechanism similar to that described by Birks' scheme).[19] This information is important for the deeper understanding of the aggregate structure and for the real-life applications of the finding. To this end, time-resolved (fluorescence) emission

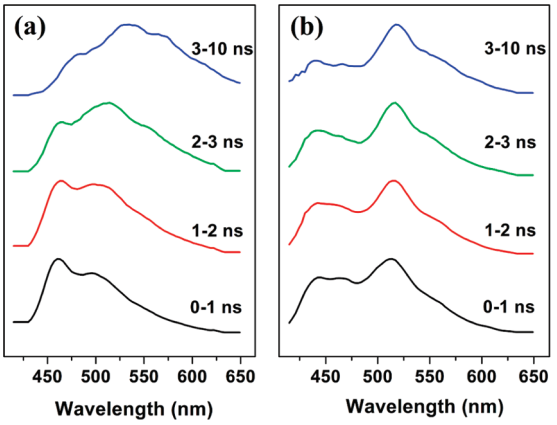

Figure 6. Time-resolved emission spectra of film **1** in air (a) and those of a controlled system of M-PPEs in THF:ethanol mixture (30:70, v/v) (b) (λ_{ex} = 380 nm).

spectroscopy measurements (TRES) were conducted for some typical systems.

TRES Measurements. Figure 6 lists the TRES spectra of film **1** in dry state recorded at different time gates (0−1, 1−2, 2−3, and 3−10 ns) and those of M-PPEs in THF:ethanol mixture (30:70, v/v) recorded at the same time gates. It is to be noted that time 0 corresponds to the time at which the excitation pulse reaches its maximum intensity. Reference to the spectra shown in Figure 6a, it is clearly seen that the profiles of the spectra at different time gates are varying from each other. The earliest time gate spectrum is characterized by the monomolecular emission of the polymer immobilized as revealed by steady-state measurement (cf. Figure 3, M-PPEs in pure THF), but this character is getting lost with the time gate moving to longer time. In contrast, a new broad emission is becoming stronger and stronger, which is the characteristic emission of the polymer in aggregated state (cf. Figure 4). The facts that no aggregate emission at the earliest time gate and increased aggregate emission appearing at later time gates indicate incontestably that the excited state of the aggregate in the film state is formed in a way similar to that described by Birks' scheme. In other words, the aggregation and disaggregation are dynamic or reversible. However, the TRES spectra of the polymer in the mixture solvent present different results (cf. Figure 6b). It is seen that the profiles of the spectra at different time gates shown in this figure are similar. The characteristic emission of the aggregate appearing at the very early time gate indicates that the aggregate is dominantly formed before the excitation and that it follows a mechanism (static aggregate) different from Birks' scheme. The less intensity of the monomolecular emission in the later time gate is mainly due to its faster decay or short lifetime. It is the dynamic nature of the aggregation of the polymer in film state that lays the foundation for sensing application, an important application as will be presented later. The differences observed for M-PPEs in two different states may be understood by considering the peculiarity of molecules at interfaces. It is known that in physics an interface can be considered as an inherent perturbation to the inversion symmetry of space and thereby introduces a new spatial director for molecules confined in it.[1d,2,20] This may magnify the minor structural differences that have negligible influences in a homogeneous medium when the molecules are confined in an interface. It is surmisable that the finding described above is of great importance for extending the sensing applications of CPs, of which synthesis and immobilization are not easy to be conducted.

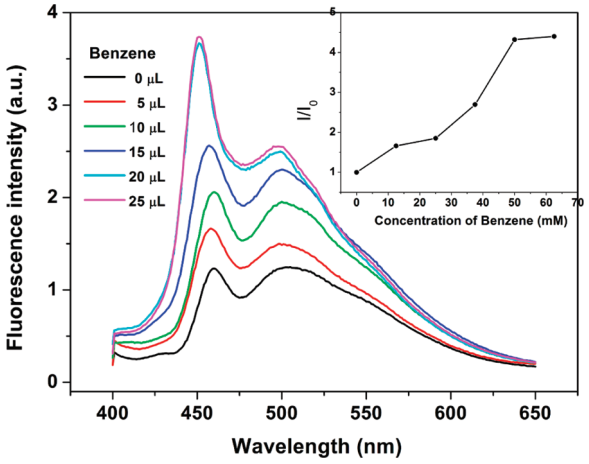

Figure 7. Fluorescence emission spectra of film **1** in benzene vapor of different densities (λ_{ex} = 380 nm). Inset is the plot of I/I_0 measured at 450 nm against the density of the benzene vapor.

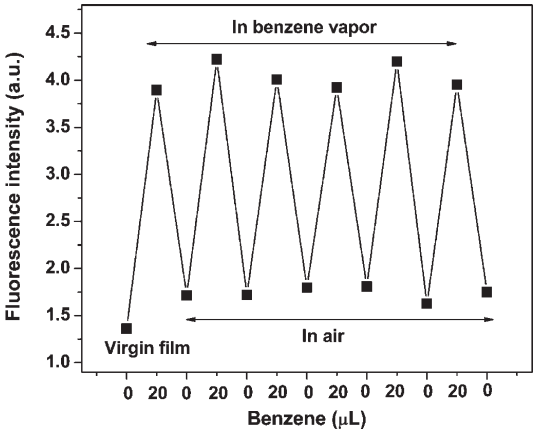

Figure 8. Reversibility of the response of film **1** to the presence of benzene vapor (λ_{ex} = 380 nm, λ_{em} = 500 nm).

Response of Film 1 to Benzene. Figure 7 shows the fluorescence emission spectra of film **1** in the presence of benzene vapor of different densities. It is seen that the intensity of the monomolecular emission increased significantly and blue-shifted a few nanometers along with increasing the density of the vapor. However, the emission does not increase further when the density of the benzene vapor exceeds a certain value (50 mmol/L). The sensitization of benzene to the fluorescence emission of the film can be understood by considering the fact that benzene is a good solvent for the polymer. In other words, the film is wettable in benzene, and thereby the balance of aggregation to disaggregation moves to the latter side, as demonstrated by the increase in the monomolecular emission. Drying of the film leads to rebuilding the original profile of the fluorescence emission. This process can be repeated for many times, and the results are depicted in Figure 8. The measurements have been conducted at room temperature, and 20 μL of benzene was used to build an organic environment (50 mmol/L) in a sealed cell. Before each measurement, the solvent was injected into a standard cell, in which the film was allied on one side. A stable emission was reached within 1 min, and the intensity of the emission was recorded. Removal of the organic vapor was realized by gently blowing the film and the cell with a nitrogen stream.

It is to be noted that the film is not only responsible to benzene vapor but also to other organic vapors, including

toluene, THF, chloroform, dichloromethane, etc. In contrast, acetone, methanol, ethanol, and water barely have any influence on the emission of the film.

To confirm the function of the side chains to the performance of film **1**, film **2** was specially fabricated, in which PPEs, possessing the same backbone as M-PPEs but with no side chains, was utilized as the fluorescent polymer instead of M-PPEs. The response of this film to benzene vapor was also evaluated, and the result is shown in Figure S6. It is seen that, compared with film **1**, benzene vapor shows little effect on the fluorescence emission of the film, indicating that the side chains did have played a crucial role to the precious performance of film **1**.

The detection limit of the film to benzene vapor was also determined by employing a standard method as described in the Supporting Information, and the result is 1.3 mmol/L.

Response of Film 1 to Mixed Solvents. It is imaginable that film **1** can be also used for sensing the compositions of some mixture solvents provided each of them consists of a "good solvent" and a "poor solvent", and the two solvents are fully miscible. As an example, Figure 9 shows the reversible response of film **1** to the changes of the compositions of the THF−ethanol mixture solvent.

Theoretical Simulation of the Aggregation Behavior. To make a deeper understanding of the aggregation to disaggregation process of the conjugated polymers immobilized on the glass plate surface, molecular dynamics (MD) were employed to simulate the possible structures of M-PPEs in different atmospheres, of which one is vacuum and another is THF.

To be simple, only the dependence of the distance between the ring plains of two OPE5, which is a model compound of M-PPEs with only 5 monomer units, molecules, and the length of the side chains of the molecules on the medium nature was simulated. The results are shown in Figure 10. It is seen that in vacuum the distance between the two molecules is about 3.2 Å, but the distance increases to 4 to 5 Å when the medium changes to THF, a good solvent for the polymer, a result in support of the findings that poor solvent or medium results in more emission from aggregated state of the polymer, but good solvent or medium results in more emission from lonely or free state of the polymer. Furthermore, the average length of the side chains of the polymer also depends upon the nature of the medium. As expected, replacing vacuum with good solvent, THF, of the polymer results in significant extension of the side chains, a result reveals the reason why the distance between the ring plains of the two molecules increases when their medium is changed to good solvent. This tentative conclusion is supported by the result from another simulation. At this time, OPE5′ was employed as a model polymer, of which no side chains were attached. The results are shown in Figure S7. It is clearly seen that medium nature shows little effect upon the distance between the two molecules, in support of the statement that side chain plays important role for the sensitivity of M-PPEs to its medium.

Conformational Behavior of Film 1 in Both Dry and Wet States. The unusual rich and colorful fluorescence behaviors of film **1** in both dry and wet states have been experimentally and theoretically studied and are schematically shown in Scheme 2. It can be seen that each state in solution or vapor corresponds to a specific dry state provided a freezing drying method is used to prepare the dry films. It is believed that only in this way that the conformations of the polymers immobilized on the substrate surface can be farthest maintained during the elimination of the solvent or vapor. According to the results shown in Figures 7−10, it should be not difficult to understand that "a", "b", and "c" stand for the possible conformations of the polymers of film **1** when it is put in a "poor", a "good", or a mixture solvent or vapor (two miscible solvents or vapors, one "good" + one "poor"), respectively. As demonstrated already, one of the three states can be transformed into another by simply changing the solvent or vapor as indicated in the Scheme. Furthermore, "a′", "b′", and "c′" stand for conformations of film **1** in dry state corresponding to "a", "b", and "c", respectively.

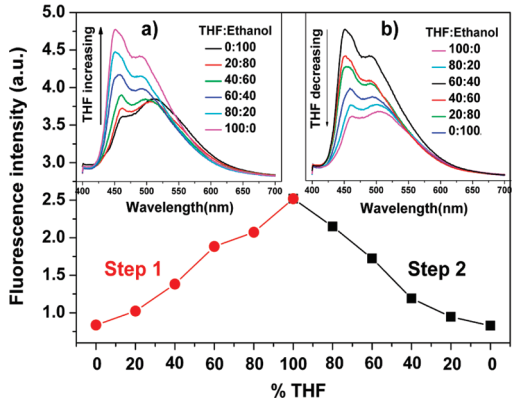

Figure 9. Plot of the fluoroescecne intensity (451 nm) of film **1** as a function of the composition of THF:ethanol mixtures. Insets: fluorescence spectra of film **1** in the mixture solvents (λ_{ex} = 380 nm). Notes: step 1: THF increases; step 2: THF decreases.

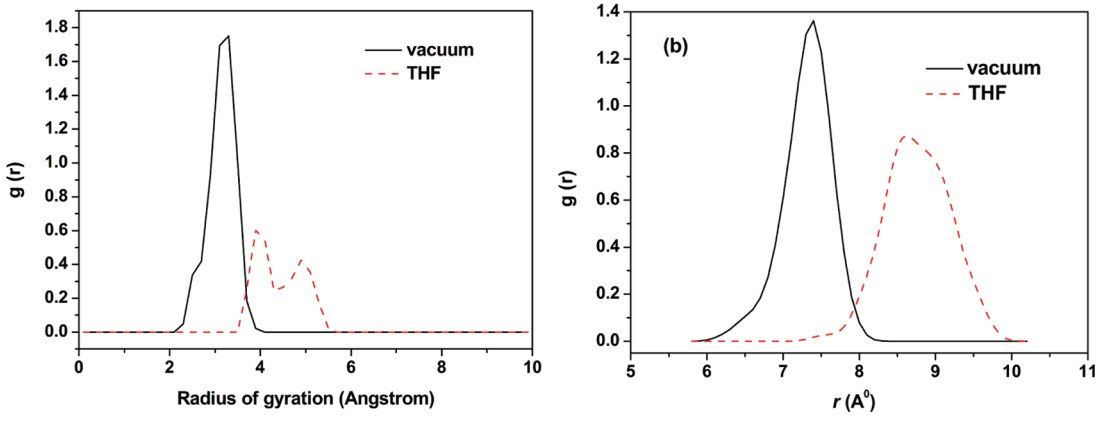

Figure 10. Radial distribution function (RDF) of OPE5 in vacuum and THF: (a) center-to-center distance between two OPE5 molecules and (b) the side chain length of OPE5.

Scheme 2. Schematic Representation of the Conformations of Film 1 in Different Conditions and the Relationships among Them

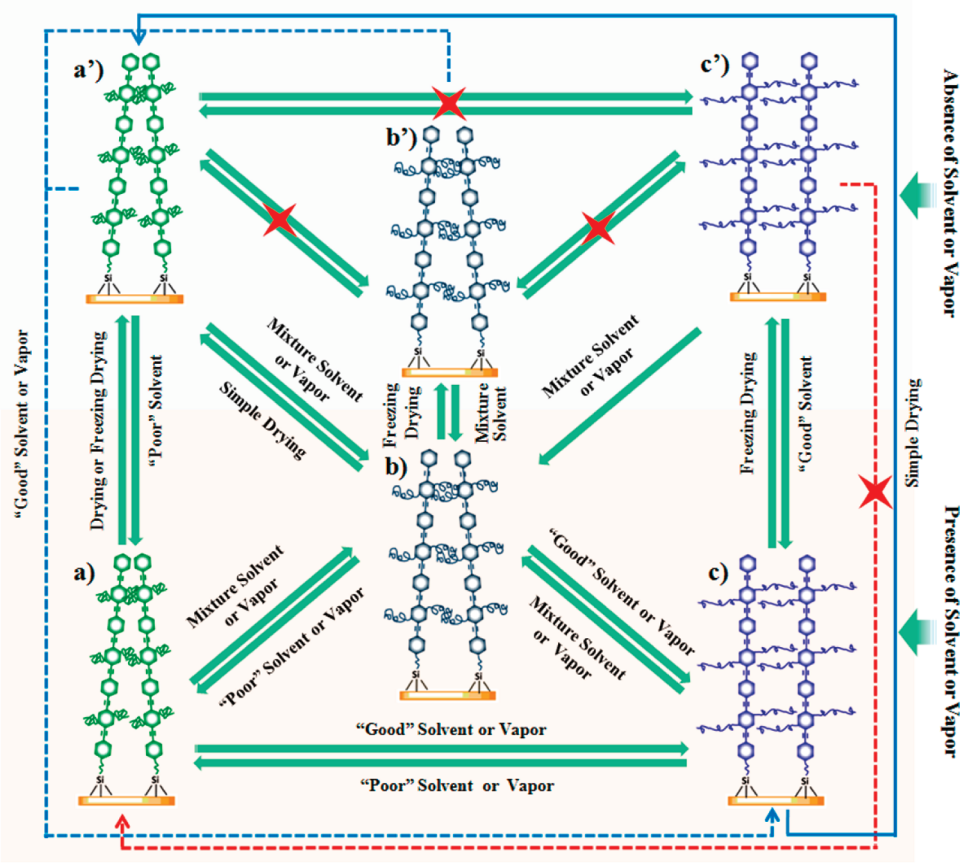

The tentative hypothesize is greatly supported by the results from fluorescence emission measurements (cf. Figure S8). Upon inspection of the figure, it is seen that both intensities and profiles of the emissions are different from each other. Furthermore, state a′ can be changed into state a, and similarly, b′ to b, and c′ to c, provided they are put in a suitable ambience or solvent as indicated in the Scheme 2. Clearly, fully understanding of the relationships shown in the scheme is meaningful for searching new applications of the film as fabricated. As an example, some molecule logic gates can be generated as described below.[21]

Logic Gates Studies. As one of molecular devices, the fluorescent logic gates based upon covalent immobilization of CPs on solid surface play a pivotal role not only because they can simultaneously treat multiple inputs but also because they can provide the chemical stability and suitability for practical applications.[22] Therefore, some logic gates based upon film **1** were principally generated. On the basis of the results shown in Figures 7 and 9, it is clear that the emission of film **1** can be reversibly modulated by changing the identity of its medium both in solution and in air. As examples, a molecular INH gate and an OR gate are presented in Figure 11 and Figure S9, respectively. The truth table for the INH gate is shown in Figure 10b, in which THF (input1) is 0 mL (low, binary 0) or 1.5 mL (high, 1) and ethanol (input2) is 0 mL (low, binary 0) or 1.5 mL (high, 1). Herein we regard a fluorescence intensity of 1.75 as the threshold value and the output = 0 when the intensity of the emission at 450 nm is low (< 1.75), whereas the output = 1 when the intensity of the emission is high (> 1.75). Thus, a strong fluorescence signal of the film is observed when THF alone is present. In contrast, a weak fluorescence is obtained

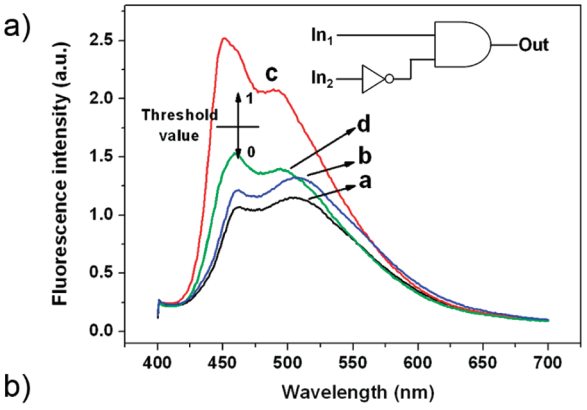

	Input$_1$(THF)	Input$_2$(Ethanol)	Output (Fluorescence Intensity)
a	0	0	0 (0.8)
b	0	1	0 (0.9)
c	1	0	1 (2.5)
d	1	1	0 (1.38)

Figure 11. Fluorescence spectra of film **1** without or with presence of THF and/or ethanol. The truth table and scheme for an INH logic gate (THF: 1.5 mL; ethanol: 1.5 mL; a: no input; b: ethanol; c: THF; d: ethanol + THF).

when ethanol is present. Namely, only input1 = 1 results in output = 1. This resulting pattern mimics the function of an electronic INH gate with a low output state occurring in the simultaneous presence of the two inputs. Similarly, an OR logic gate can be also generated. The details can be found in

Figure S9 and the relevant descriptions in the Supporting Information. It is to be noted that this should be the first report of fluorescent molecular logic gate based upon immobilized CPs.

Conclusions

In summary, a novel stimulus-responsive, CP-based fluorescent film has been developed by chemical attaching a structurally modified CP onto a glass plate surface via a short spacer. The film shows reversible, supersmart response to some external stimulus, such as presence of toxic volatile organic solvents, including benzene, toluene, chloroform, THF, dichloromethane, etc., and changes in the compositions of suitable mixture solvents. Fluorescence and MD modeling studies revealed that the long, flexible alkyl chains have played crucial role on the smart performances of the CPs functionalized film. Interestingly, both an INH and an OR logic gates can be simply generated by employing the smart film as created. It is believed that the strategy proposed in this work may provide a new way for the design of SAMs and CP-based fluorescent sensing films.

Acknowledgment. We thank the Natural Science Foundation of China (No. 200773083, 20927001), the Ministry of Science and Technology of China (No. 2007AA03Z349), and the Department of Science and Technology of Shaanxi Province (2010ZDKG-89) for financial support.

Supporting Information Available: Details of control experiments, stability of the fluorescent film, aggregation of M-PPEs in mixed solvents, detection limit of film **1** to benzene vapor, fluorescence emission spectra of film **2** in benzene vapor, theoretical simulation of aggregation behavior, and the OR logic gate. This material is available free of charge via the Internet at http://pubs.acs.org.

References and Notes

(1) (a) George, S. M.; Yoon, B.; Dameron, A. A. *Acc. Chem. Res.* **2009**, *42*, 498–508. (b) Pischel, U. *Angew. Chem., Int. Ed.* **2010**, *49*, 1356–1358. (c) Onclin, S.; Ravoo, B. J.; Reinhoudt, D. N. *Angew. Chem., Int. Ed.* **2005**, *44*, 6282–6304. (d) Yerushalmi, R.; Scherz, A.; van der Boom, M. E. *J. Am. Chem. Soc.* **2004**, *126*, 2700–2701. (e) Han, Y.-J.; Aizenberg, J. *Angew. Chem., Int. Ed.* **2003**, *42*, 3668–3670. (f) Tokarev, I.; Motornov, M.; Minko, S. *J. Mater. Chem.* **2009**, *19*, 6932–6948. (g) Shekhah, O.; Wang, H.; Paradinas, M.; Ocal, C.; Schupbach, B.; Terfort, A.; Zacher, D.; Fischer, R. A.; Woll, C. *Nature Mater.* **2009**, *8*, 481–484.

(2) (a) Kuzmenko, I.; Rapaport, H.; Kjaer, K.; Nielsen, J. A.; Weissbuch, I.; Lahav, M.; Leiserowitz, L. *Chem. Rev.* **2001**, *101*, 1659–1696. (b) Moon, J. H.; Swager, T. M. *Macromolecules* **2002**, *35*, 6086–6089. (c) Nicholas Marshall, N.; Sontag, S. K.; Locklin, J. *Macromolecules* **2010**, *43*, 2137–2144. (d) Sontag, S. K.; Marshall, N.; Locklin, J. *Chem. Commun.* **2009**, 3354–3356.

(3) (a) Woll, C. *Angew. Chem., Int. Ed.* **2009**, *48*, 8406–8408. (b) Fischer, R. A.; Woll, C. *Angew. Chem., Int. Ed.* **2009**, *48*, 6205–6208. (c) Shekhah, O.; Wang, H.; Kowarik, S.; Schreiber, F.; Paulus, M.; Tolan, M.; Sternemann, C.; Evers, F.; Zacher, D.; Fischer, R. A.; Woll., C. *J. Am. Chem. Soc.* **2007**, *129*, 15118–15119. (d) Ito, Y.; Virkar, A. A.; Mannsfeld, S. C. B.; Oh, J. H.; Toney, M.; Locklin, J.; Bao, Z. *J. Am. Chem. Soc.* **2009**, *131*, 9396–9404. (e) Wu, X. F.; Xu, B. W.; Tong, H.; Wang, L. X. *Macromolecules* **2010**, *43*, 8917–8923.

(4) (a) Chrisstoffels, L. A. J.; Adronov, A.; Frechet, J. M. J. *Angew. Chem., Int. Ed.* **2000**, *39*, 2163–2167. (b) Ravoo, B. J. *J. Mater. Chem.* **2009**, *19*, 8902–8906. (c) Fries, K.; Samanta, S.; Orski, S.; Locklin, J. *Chem. Commun.* **2008**, 6288–6290. (d) Lv, F. T.; Fang, Y.; Blanchard, G. J. *Langmuir* **2008**, *24*, 8752–8759. (e) Ding, L. P.; Kang, J. P.; Lv, F. T.; Gao, L. N.; Yin, X.; Fang, Y. *Thin Solid Films* **2007**, *515*, 3112–3119.

(5) (a) Veen, N. J.; Flink, S.; Deij, M. A.; Egberink, R. J. M.; Veggel, F. C. J. M.; Reinhoudt, D. N. *J. Am. Chem. Soc.* **2000**, *122*, 6112–6113. (b) Crego-Calama, M.; Reinhoudt, D. N. *Adv. Mater.* **2001**, *13*, 1171–1174.

(6) (a) Gao, L. N.; Fang, Y.; Wen, X. P.; Li, Y. G.; Hu, D. D. *J. Phys. Chem. B* **2004**, *108*, 1207–1213. (b) Lv, F. T.; Gao, L. N.; Ding, L. P.; Jiang, L. L.; Fang, Y. *Langmuir* **2006**, *22*, 841–845. (c) Zhang, S. J.; Lv, F. T.; Gao, L. N.; Ding, L. P.; Fang, Y. *Langmuir* **2007**, *23*, 1584–1590.

(7) (a) Balzani, V.; Credi, A.; Venturi, M. *ChemPhysChem* **2008**, *9*, 202–220. (b) Takahashi, I.; Honda, Y.; Hirota., S. *Angew. Chem., Int. Ed.* **2009**, *48*, 6065–6068. (c) Baisch, B.; Raffa, D.; Jung, U.; Magnussen, O. M.; Nicolas, C.; Lacour, J.; Kubitschke, J.; Herges., R. *J. Am. Chem. Soc.* **2009**, *131*, 442–443. (d) Ikegami, A.; Suda, M.; Watanabe, T.; Einaga, Y. *Angew. Chem., Int. Ed.* **2009**, *48*, 372–374. (e) Gahl, C.; Schmidt, R.; Brete, D.; McNellis, E. R.; Freyer, W.; Carley, R.; Reuter, K.; Weinelt, M. *J. Am. Chem. Soc.* **2010**, *132*, 1831–1838.

(8) (a) Swager, T. M. *Acc. Chem. Res.* **1998**, *31*, 201–207. (b) McQuade, D. T.; Pullen, A. E.; Swager, T. M. *Chem. Rev.* **2000**, *100*, 2537–2574.

(9) (a) Heeger, P. S.; Heeger, A. J. *Proc. Natl. Acad. Sci. U.S.A.* **1999**, *96*, 12219–12221. (b) Lee, K.; Rouillard, J.-M.; Pham, T.; Gulari, E.; Kim, J. S. *Angew. Chem., Int. Ed.* **2007**, *46*, 4667–4670. (c) Thomas, S. W., III; Joly, G. D.; Swager, T. M. *Chem. Rev.* **2007**, *107*, 1339–1386. (d) Feng, X. L.; Duan, X. R.; Liu, L. B.; Feng, F. D.; Wang, S.; Li, Y. L.; Zhu, D. B. *Angew. Chem., Int. Ed.* **2009**, *48*, 5316–5321. (e) Kwak, G.; Lee, W.-E.; Jeong, H.; Sakaguchi, T.; Fujiki, M. *Macromolecules* **2009**, *42*, 20–24. (f) Liu, J. Z.; Zhong, Y. C.; Lam, J. W. Y.; Lu, P.; Hong, Y. M.; Yu, Y.; Yue, Y. N.; Faisal, M.; Sung, H. H. Y.; Williams, I. D.; Wong, K. S.; Tang, B. Z. *Macromolecules* **2010**, DOI: 10.1021/ma902432m.(g) Lee, W. E.; Kim, J. W.; Oh, C. J.; Sakaguchi, T.; Fujiki, M.; Kwak, G. *Angew. Chem., Int. Ed.* **2010**, *49*, 1406–1409.

(10) (a) He, G.; Zhang, G. F.; Lv, F. T.; Fang, Y. *Chem. Mater.* **2009**, *21*, 1494–1499. (b) Liu, T. H.; He, G.; Yang, M. N.; Fang, Y. *J. Photochem. Photobiol., A* **2009**, *202*, 178–184.

(11) (a) Bunz, U. H. F. *Chem. Rev.* **2000**, *100*, 1605–1644. (b) Liu, J. Z.; Lam, J. W. Y.; Tang., B. Z. *Chem. Rev.* **2009**, *109*, 5799–5867.

(12) (a) Ding, L. P.; Chi, E. Y.; Chemburu, S.; Ji, E.; Schanze, K. S.; Lopez, G. P.; Whitten, D. G. *Langmuir* **2009**, *25*, 13742–13751. (b) Satrijo, A.; Swager, T. M. *J. Am. Chem. Soc.* **2007**, *129*, 16020–16028.

(13) Swager, T. M.; Gil, C. J.; Wrighton, M. S. *J. Phys. Chem.* **1995**, *99*, 4886–4893.

(14) Ogawa, K.; Chemburu, S.; Lopez, G. P.; Whitten, D. G.; Schanze, K. S. *Langmuir* **2007**, *23*, 4541–4548.

(15) Kurth, D. G.; Bein, T. *Langmuir* **1993**, *9*, 2965–2973.

(16) Lv, F. T.; Gao, L. N.; Li, H. H.; Ding., L. P.; Fang, Y. *Appl. Surf. Sci.* **2007**, *253*, 4123–4131.

(17) Kim, J.; McQuade, D. T.; McHugh, S. K.; Swager, T. M. *Angew. Chem., Int. Ed.* **2000**, *39*, 3868–3872.

(18) Wang, H.; Fang, Y.; Cui, Y. L.; Hu, D. D.; Gao, G. L. *Mater. Chem. Phys.* **2002**, *77*, 185–191.

(19) (a) Birks, J. B. *Photophysics of Aromatic Molecules*; Wiley: London, 1970. (b) Lakowicz, J. R. *Principles of Fluorescence Spectroscopy*; Plenum Press: New York, 2006.

(20) Benitez, I. O.; Bujoli, B.; Camus, L. J.; Lee, C. M.; Odobel, F.; Talham, D. R. *J. Am. Chem. Soc.* **2002**, *124*, 4363–4370.

(21) (a) Magri, D. C.; Brown, G. J.; McClean, G. D.; de Silva, A. P. *J. Am. Chem. Soc.* **2006**, *128*, 4950–4951. (b) Tang, Y. L.; He, F.; Wang, S.; Li, Y. L.; Zhu, D. B.; Bazan, G. C. *Adv. Mater.* **2001**, *18*, 2105–2110. (c) Onoda, M.; Uchiyama, S.; Ohwada, T. *Macromolecules* **2007**, *40*, 9651–9657.

(22) (a) Mu, L. X.; Shi, W. S.; She, G. G.; Chang, J. C.; Lee, S. T. *Angew. Chem., Int. Ed.* **2009**, *48*, 3469–3472. (b) de Silva, A. P.; James, M. R.; Mckinney, B. O. F.; Pears, D. A.; Weir, S. M. *Nature Mater.* **2006**, *5*, 787–790.